

DRAM Errors and Cosmic Rays: Space Invaders or Science Fiction?

1st Isaac Boixaderas
Barcelona Supercomputing Center
Barcelona, Spain
isaac.boixaderas@bsc.es

2nd Jorge Amaya
European Space Agency
Hesse, Germany
jorge.amaya@esa.int

3rd Sergi Moré
Barcelona Supercomputing Center
Barcelona, Spain
sergi.more@bsc.es

4th Javier Bartolome
Barcelona Supercomputing Center
Barcelona, Spain
javier.bartolome@bsc.es

5th David Vicente
Barcelona Supercomputing Center
Barcelona, Spain
david.vicente@bsc.es

6th Osman Unsal
Barcelona Supercomputing Center
Barcelona, Spain
osman.unsal@bsc.es

7th Dimitris Gizopoulos
University of Athens
Athens, Greece
dgizop@di.uoa.gr

8th Paul M. Carpenter
Barcelona Supercomputing Center
Barcelona, Spain
paul.carpenter@bsc.es

9th Petar Radojković
Barcelona Supercomputing Center
Barcelona, Spain
petar.radojkovic@bsc.es

10th Eduard Ayguadé
Barcelona Supercomputing Center
Barcelona, Spain
eduard.ayguade@bsc.es@bsc.es

Abstract—It is widely accepted that cosmic rays are a plausible cause of DRAM errors in high-performance computing (HPC) systems, and various studies suggest that they could explain some aspects of the observed DRAM error behavior. However, this phenomenon is insufficiently studied in production environments.

We analyze the correlations between cosmic rays and DRAM errors on two HPC clusters: a production supercomputer with server-class DDR3-1600 and a prototype with LPDDR3-1600 and no hardware error correction. Our error logs cover 2000 billion MB-hours for the MareNostrum 3 supercomputer and 135 million MB-hours for the Mont-Blanc prototype. Our analysis combines quantitative analysis, formal statistical methods and machine learning.

We detect no indications that cosmic rays have any influence on the DRAM errors. To understand whether the findings are specific to systems under study, located at 100 meters above the sea level, the analysis should be repeated on other HPC clusters, especially the ones located on higher altitudes. Also, analysis can (and should) be applied to revisit and extend numerous previous studies which use cosmic rays as a hypothetical explanation for some aspects of the observed DRAM error behaviors.

Index Terms—Memory system, Reliability, Cosmic rays

I. INTRODUCTION

In large-scale compute clusters, main memory is one of the principal causes of hardware failures [1]–[5]. These failures are especially costly in high-performance computing (HPC) systems, where a single tightly-coupled job may execute for days on thousands of nodes. If one of these nodes fails, the whole job is terminated. It is therefore important to

understand memory system reliability, as it is an important limit on the ability to scale to larger systems.

Many studies analyze DRAM errors in the field. One of the potential causes of DRAM errors are cosmic rays. Various industrial studies performed between the 1970s and early 1990s [6], [7] demonstrate that some of these particles have sufficient energy to penetrate Earth’s atmosphere down to the sea level, through the ceiling of the multistory buildings and induce DRAM bit-flips [8]. Since then, the community has accepted that cosmic rays are a plausible cause of DRAM errors in HPC systems [2], [3], [9]–[15].

Some studies go a step further and suggest that cosmic rays could explain some aspects of the observed DRAM error behavior, such as the higher error rates in the top rack chassis [16] or in the clusters geographically located at higher altitudes [16]–[18]. The studies also suggest that some (but not all) DRAM devices are susceptible to transient faults from cosmic ray strikes, and that this susceptibility highly varies between the device manufacturers [18]. The cosmic rays are also considered a potential cause of failures with no prior symptoms and no relevant information in the system logs [12].

To the best of our knowledge, only one previous study has analyzed the relationship between DRAM error rates and the cosmic rays intensity. El-Sayed and Schroeder [19] analyze error logs from HPC clusters at Los Alamos National Lab and conclude that rates of uncorrected DRAM errors are not associated with cosmic rays intensity. The authors find this result unexpected and provide one possible explanation

for it: while increasing cosmic rays might lead to a higher rates of DRAM corruptions, the types of corruption caused by those events might usually be corrected with the built-in error correction codes. This reasoning is aligned with the idea that transient errors typically lead to a single-bit data corruption [10].

Our study describes the underlying sources of high-energy cosmic rays, explains which particles should be observed, and points to the publicly-available logs from reliable measurement facilities (Section II). We study the DRAM errors of MareNostrum 3 large-scale production system and mid-scale Mont-Blanc prototype, which does not support memory error correction in hardware. The systems are located in the same geographical location, in Barcelona (Spain), and the errors are logged in overlapping time-periods. The MareNostum 3 logs cover 2000 billion MB-hours of server-class DDR3-1600 DIMMs during which we detected 4.5 million corrected and 71 uncorrected DRAM errors (Section III). In the Mont-Blanc prototype, we collected over 25 million memory errors during the 135 million MB-hours production of mobile LPDDR3-1600 chips (Section IV).

We explore a correlation between the cosmic rays intensity and number of corrected, transient corrected and uncorrected DRAM errors (Section V and VI). We also use statistical tests to study whether the error rates have different distributions during periods of elevated cosmic ray activity, e.g. above 90th or 99th neutron count percentile (Section VII). Our exploration covers a vast number of tests with numerous error categories, time windows and system scopes. We also examine whether machine learning methods for DRAM error prediction would be enhanced if they considered the neutron count measurements (Section VIII). Finally, we apply the presented methodology to verify and question some findings from previous studies (Section IX).

We hope that the insights gained in this study and the presented methodology will become a standard for any future analysis of the relationship between cosmic rays and DRAM errors in the field. The analysis can (and should) be also applied to revisit and extend numerous previous studies which use cosmic rays as a hypothetical explanation for some aspects of the observed DRAM error behaviors. Our study motives, guides and enables a follow-up research on this frequently mentioned, but insufficiently studied phenomenon.

II. COSMIC RAYS

A. Background

Cosmic rays are high-energy particles that originate from outer space. They normally come from supernovae or other energetic events in the galaxy, and occasionally come from the Sun during periods of high solar activity. When cosmic rays enter the Earth’s atmosphere, they produce a cascade of secondary particles which can reach the Earth’s surface and even penetrate underground. The particles hitting the DRAM chips can alternate the cell charge and corrupt the stored data, causing DRAM errors.

The density of the atmosphere decreases exponentially with altitude, providing less shielding at higher altitudes. This results in a greater flux of secondary particles and an increased probability of errors caused by cosmic rays at higher elevations [7], [8], [20]. A common belief is that cosmic rays are also a plausible cause of DRAM errors in datacenters, especially if they are located on high altitudes. This belief, however, is not supported by any large-scale field study.

B. Data collection

From all the cascading elements produced by cosmic rays, neutrons are the most commonly observed at ground level. Their flux can be measured with specialized **neutron monitors**, ground-based detectors that measure the neutrons that reach the Earth’s surface. Rare solar events that produce very high-energy particles can also generate secondary cascades in the atmosphere, which can be detected by neutron monitors. The Neutron Monitor Database [21] provides public access to neutron count logs from more than 50 neutron monitors located all over the world, most of them in the northern hemisphere.

To quantify the impact of cosmic rays on HPC cluster failure rates, users can correlate the system error logs with the neutron counts from a monitor. The monitor should be selected based on the distance and the altitude difference with respect to the HPC facility. If various nearby neutron monitors are available, the users should compare their measurements to ensure that they are representative of the cosmic ray activity in the region. The exact number of neutron counts reported by these monitors can vary, but their correlation should be high.

We considered the cosmic ray logs from two neutron monitors. The first one is located in Guadalajara (Spain), 470 km southwest of Barcelona, situated at an altitude of 708 meters [22]. The second one is in Rome (Italy), 870 km east of Barcelona and located close to sea level [23], as the MareNostrum supercomputer and the Mont-Blanc prototype. During the period of our DRAM error logs, we observed a high correlation coefficient between neutron counts from Guadalajara and Rome. This correlation, together with the geographic positioning of Guadalajara and Rome neutron monitors, both relatively close to Barcelona but on opposite sides, indicate that the considered neutron monitor measurements are likely representative of the general cosmic rays in our region.

Because of proximity, we used the Guadalajara cosmic ray logs. To ensure that the measurements accurately reflect cosmic ray activity, we use data corrected for pressure and instrumental factors.¹ Corrections for instrumental changes, such as modifications of the building and the measurement equipment, are necessary to maintain data consistency. Also, the atmospheric pressure correction is important because higher atmospheric pressure increases the air mass above the detector, reducing the detected neutron flux.

Solar cycles are periodic fluctuations in solar activity, lasting approximately 11 years. During the period of our logs, we

¹In the Neutron Monitor logs, this is referred to as efficiency correction.

were in a descending phase of a Solar cycle which began in December 2008 and ended in December 2019. During periods of high solar activity, the solar wind acts as a shield against galactic cosmic rays from sources beyond the Sun and prevent them to reach the Earth [24]. A clear anti-correlation has been observed between the activity of the solar cycle and measurements, on the ground and in space, of galactic cosmic rays. This is visible in the neutron counts, which moderately increase during the observation period (see Section V-A).

III. MARENOSTRUM 3 DRAM ERRORS

A. MareNostrum 3 supercomputer

The MareNostrum 3 error logs cover a period of more than two years, from October 2014 to November 2016, during which we detected 4.5 million corrected and 71 uncorrected DRAM errors.² The supercomputer was located in Barcelona (Spain), 100 meters above the sea level, in a stone-walls chapel with a ceramic tiles roof. At the time, MareNostrum 3 was one of the six Tier-0 (largest) HPC systems in the Partnership for Advanced Computing in Europe (PRACE) [25]. It comprised 3056 compute nodes, each with two eight-core Intel Sandy Bridge-EP E5-2670 sockets with a 2.6 GHz nominal clock frequency. We use the logs from the compute nodes only, excluding the login and test nodes which are not part of the same monitoring infrastructure and whose failures do not impact large-scale compute jobs.

The MareNostrum 3 compute nodes included more than 25,000 DDR3-1600 DIMMs from all three major manufacturers: 6694, 5207 and 13,419 DIMMs from *Manufacturer A*, *B* and *C*, respectively. The manufacturers have been anonymized to protect the interested parties. MareNostrum 3 DIMMs were built in three different DRAM technologies: $\overline{3x}$ nm, $\overline{2y}$ nm and $\overline{2z}$ nm. We are allowed to show only the first of two digits of the nanometer technology and their relative order: $\overline{3x}$ nm > $\overline{2y}$ nm > $\overline{2z}$ nm. During the observation period we collected measurements on more than 2000 billion MB-hours. The main workloads executed on MareNostrum 3 were large-scale scientific HPC applications and the system utilization typically exceeded 95%.

MareNostrum 3 employed a Chipkill ECC scheme, which could correct all errors coming from a single x4 device. For x8 devices, the ECC can correct up to 4-bit errors coming from the same DRAM chip. The ECC check is performed on each application memory read and by a patrol scrubber which periodically traverses the whole physical memory and performs an ECC check on each location.

During production, any DIMM that showed early signs of failure was flagged by a pre-failure alert and retired by the system administrators. This action was recorded in the system log together with the date and time. Over the two-year period analysed by this paper, 51 DIMMs were retired for this reason.

²The log also contains 262 over-temperature DRAM errors, but they are not analyzed because they are unrelated to the cosmic ray activity.

B. Data collection

Corrected errors (CEs) were logged by a daemon, based on the mcelog Linux kernel module [26], that periodically extracts information about corrected errors from the CPU machine-check architecture (MCA) registers [26]. Each corrected error was recorded in a log file, which specifies the error timestamp, node and DIMM id, and the physical location of the error in the DIMM including rank, bank, row and column. The log entry also indicates whether correction was done during an application memory read or by patrol scrubbing.

The daemon accessed the MCA registers with a period of 100 ms, which was the shortest time interval that caused negligible overhead to the production applications. If more than one error occurred in a 100 ms time interval, the MCA registers record the number of errors, but only provide detailed information for one error in the interval. Our logs therefore specify the exact total number of corrected errors and provide detailed error information for a subset of the errors. Increasing the sampling frequency would increase the number of errors with detailed information, but also increase the performance overhead of the error logging daemon. Previous studies perform similar readings of the memory error registers with a period of a few seconds [16], [18], [27] or once per hour [10].

Our analysis covers both, **transient** and **non-transient** CEs. Transient CEs are frequently considered to be caused by temporary environmental factors, such as cosmic ray strikes [4], [10], [18], [27]. We consider an error to be transient if, during the entire observation period, the error occurred only once in a given cell and no other errors occurred in the same row or column [4].

Uncorrected errors (UEs) were logged by IBM firmware [28], which is part of the MareNostrum 3 monitoring software. For each uncorrected error, the log specifies the DIMM that failed and the cause of the error, i.e. whether it occurred during an application memory read or patrol scrubbing. Finally, the log records UE warnings generated when memory modules are throttled to prevent an over-temperature condition and when the correctable ECC logging limit has been reached.

IV. MONT-BLANC DRAM ERRORS

A. Mont-Blanc prototype

The prototype was located in Barcelona (Spain), in the same area and altitude as MareNostrum, 100 meters above the sea level. The system was deployed in a brick building with a concrete roof. The Mont-Blanc prototype comprised 1080 nodes based on the Samsung Exynos 5250 mobile system-on-chip (SoC) [29]. Each SoC integrated two 1.7 GHz Arm Cortex-A15 cores, one on-chip Mali-T604 GPU and 4 GB of LPDDR3-1600. All memory devices are from the same manufacturer. The objective of the Mont-Blanc prototype was to explore the suitability of high-performance computing on hardware initially targeting mobile devices. Therefore, the deployed LPDDR3 main memory included no error detection or correction mechanisms.

B. Data collection

Mont-Blanc error logging lasted for over a year, February 2015 to February 2016, which is within the time-frame of the MareNostrum logs. It monitored over 4.2 million node-hours, 135 million MB-hours of LPDDR3-1600, and logging over 25 million memory errors [30]. DRAM errors were logged with a software daemon running an infinite loop that traverses the whole available system memory. In each node, the daemon allocated approximately 3 GB of main memory, while the rest was dedicated for the OS and other system software. The daemon was first writing a specific value into each memory location, and then, in the next loop iteration, was checking whether the memory still contained the correct data. If this was not the case, the tool recorded the memory error location and the number of corrupted bits. Since the daemon memory utilization was significant, it was executed only when the nodes were not running any user job. For this reason, the total amount of memory scanned depended on the prototype utilization, which varied in time. To account for this, we normalize the number of DRAM errors per amount of scanned memory in that specific time. The Mont-Blanc error-logging framework was set by Bautista et al. [30]. Our analysis is based on the data reported in the original study.

V. TIMELINE ANALYSIS

We first examine the timelines of the DRAM error logs and neutron counts to understand the general trends and overall behavior. This analysis helps to put into context the correlation analysis of Section VI.

A. Neutron counts

Figure 1 shows neutron counts per second recorded by the Guadalajara neutron monitor from October 2014 to November 2016, the period corresponding to the DRAM error logs of MareNostrum 3. The overall neutron count range in this period is representative of the complete operational neutron monitor data spanning from 2012 to 2024. We plot the neutron counts per second averaged by hour and by month. The hourly data is the finest granularity that provides a readable plot. We also see some variation within the cycle, and some peak behavior, e.g. negative peaks in January and July 2015, and a positive peak in November 2016. Finally, we also see a general trend of increasing monitor counts over time, especially after August 2015. This increasing trend is confirmed with the trend-line showing monthly neutron averages, and it may be attributed to decreasing solar activity in this period, as discussed in Section II-B.

B. DRAM errors

Figure 2a shows the **MareNostrum corrected errors (CEs)** hourly and monthly occurrences between October 2014 and November 2016. On most hours there are up to 100 corrected errors, but on a few hours the number of errors is large, up to about 10,000. The results suggest that we should further explore a potential alignment between the neutron count and error peaks. Comparison of the neutrons and CEs monthly

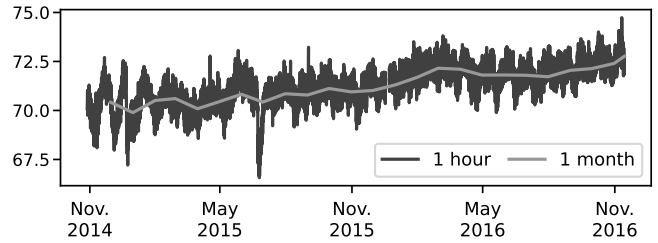
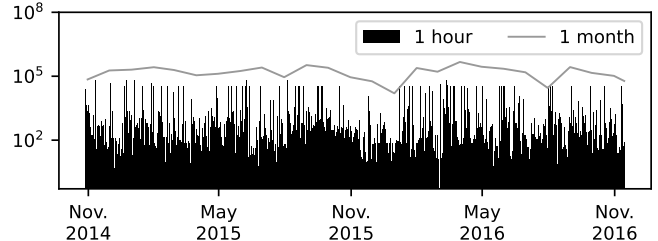
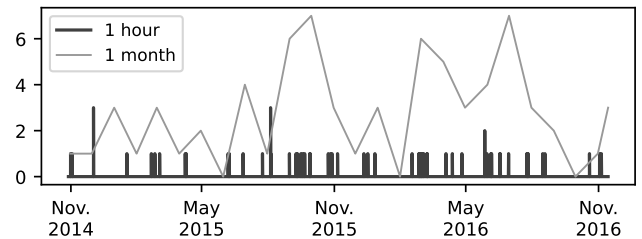


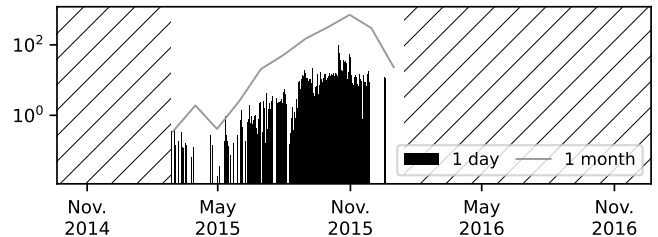
Fig. 1: Neutron counts per second. Hour and month averages.



(a) MareNostrum 3: Total corrected errors per hour and per month.



(b) MareNostrum 3: Total uncorrected errors per hour and per month.



(c) Mont-Blanc: Total errors per day and per month.

Fig. 2: DRAM errors over time. MareNostrum 3 production supercomputer and Mont-Blanc prototype.

trend-lines, Figures 1 and 2a, detects no obvious correlation between these two variables. We repeat this analysis focused only on the transient CEs, and we reach the same conclusions.

Figure 2b shows the number of **uncorrected MareNostrum DRAM errors (UEs)** per hour and per month, across all DIMMs. In most hours we detect no errors, on a few hours we detect one error, and very occasionally we detect two or three errors. In total during the observation period of 25 months we detect only 71 errors. Regarding the monthly values, we detect somewhat higher UE rates in the period June 2015 to June 2016, which does correspond to above-average neutron counts. However, we also detect some of the lowest UE numbers in the last months of the study, which is

the period of the highest cosmic rays intensity. Overall, the visual comparison of the neutron and UE trend-lines detects no obvious correlation.

Figure 2c depicts the number of errors per day and per month for the Mont-Blanc system, normalized to the amount of scanned main memory. The timescale (x -axis) is aligned with the neutron counts measurements in Figure 1 and the hatched section of the chart indicates the time period for which we do not have Mont-Blanc error logs. From May to November 2015, we see a significant monotonic increment of the error rates, well correlated with the neutron counts. However, the correlation is low at the beginning and the end of the Mont-Blanc logs. This is especially pronounced in the last three months, November 2015 to February 2016, in which the neutron counts continue to increase, while the error rates drop by an order of magnitude.

VI. CORRELATIONS

Next, we further explore the correlation between the neutron counts and DRAM error rates.

A. Methodology

First, we use a visual correlation between the neutron counts and the total number of DRAM errors detected in the same time period. Second, we apply the Kendall test [31] to explore correlation for a large number of error categories.³ We perform statistical tests on all combinations of the error categories, time windows, and system scopes listed in Table I (MareNostrum 3) and Table II (Mont-Blanc). For MareNostrum supercomputer, this leads to a vast number of correlation tests: 1,764,096 for uncorrected and 10,584,576 for corrected errors.⁴ In Mont-Blanc error logs contain much less information, leading to only 21 error categories.

For each experiment, the Kendall’s test returns a correlation coefficient between -1 (strong inverse correlation) and +1 (strong direct correlation). The test also detects cases in which the correlation cannot be tested. If all values of one variable are identical, e.g. zero detected DRAM errors, it is impossible to rank them meaningfully, and there is no basis to determine concordance or discordance with the cosmic rays intensity. Finally, the Kendall’s test returns a p -value that quantifies the correlation significance. A large number of applied tests increases the probability that some tests incorrectly suggest correlation significance (i.e. low p -values). To minimize this

³Kendall’s test assesses the strength and direction of the association between two variables by measuring the ordinal association between them. We also considered Pearson correlation and Spearman’s rank correlation. Pearson correlation is disregarded because it requires normal data distribution and a linear relationship between the two variables. As Kendall’s coefficient, Spearman’s correlation is a rank-based non-parametric test, so it can be applied to our analysis. We selected the Kendall correlation measure because it is more robust than Spearman’s rank correlation [32].

⁴For example, for uncorrected errors, there are four time-windows, four manufacturer categories, three error types, and four technologies for a total of 192 combinations. The main increase in tests comes from 9188 different system scopes. The tests are applied to the whole system, but also individually for each of the 37 racks, 3050 nodes, and 6100 sockets ($1 + 37 + 3050 + 6100 = 9188$).

TABLE I: MareNostrum 3 error categories, time-windows and system scopes.

MareNostrum uncorrected and corrected errors	
Manufacturers	A, B, C , All
DIMM technology	$3x$ nm, $2y$ nm, $2z$ nm, All
Time window	Hour, day, week, month
System scope	Whole system, 37 racks, 3050 nodes, 6100 sockets
MareNostrum corrected errors	
Transient vs. Non-transient	Transient, Non-transient, All
Error type	Memory read, Patrol scrub, All
Single/multi-cell	Single-cell, Multi-cell, All
CEs vs. DIMMs	Total number of CEs, Number of DIMMs with at least one CE
MareNostrum uncorrected errors	
Error types	Uncorrected ECC, Scrub failed, All

TABLE II: Mont-Blanc error categories and time-windows.

n-bit error	1, 2, 3, 4, 5, 6+ bits, All
Time window	Day, week, month

likelihood we apply the Benjamini–Yekutieli false discovery rate method [33].

B. Visual correlation

Figure 3 shows averaged neutron counts per second (x -axis) and the number of memory errors recorded in the corresponding time period (y -axis). As in the rest of the paper, the Mont-Blanc error counts are normalized with the amount of scanned memory. The figures plot the data for the whole system, 3056 MareNostrum 3 nodes and 1080 Mont-Blanc nodes. We use a gray heat-map to show the number of observations with a given error and neutron count. To cover a large range of MareNostrum CEs per hour, the y -axis and the heatmap in Figure 3a use a log scale.

Overall, we find no correlation that can be observed with the naked eye. We repeat the experiments for MareNostrum transient corrected errors, and we reach the same conclusion. All three charts show a higher density between 70 and 72 neutron counts per second because this is the most frequent neutron count range during the time of the study.

C. Statistical tests

In **MareNostrum** analysis, numerous error categories, time windows and system scopes lead to a vast overall exploration space. However, the nature of the DRAM errors and some practical limitations, hugely reduce the number of practical correlation tests: from 1,764,096 to 2352 for uncorrected, and from 31,753,728 to 671,404 for corrected errors. There are three main reasons for this reduction. First, most of the nodes experienced no DRAM errors: 62% experienced no CEs, and 99% no UEs. For these nodes, there is no basis to determine

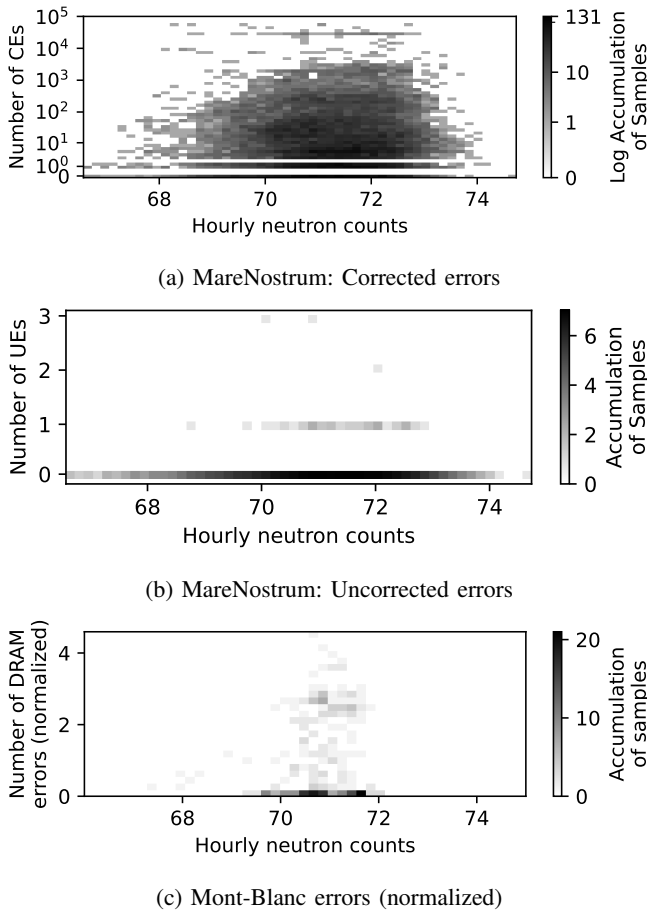


Fig. 3: Neutron counts (x -axis) and the number of DRAM errors in the corresponding time period (y -axis). Bare-eye analysis detects no correlations.

DRAM error concordance or discordance with the neutron counts. Also, not all possible categorical combinations are present in practice. For example, each MareNostrum node comprises DIMMs from the same manufacturer and technology. If a given node experiences DRAM errors, it can be tested only for this specific manufacturer–technology pair, not for all possible combinations of these two parameters. Finally, many of the error log inputs are incomplete, with some fields that are omitted.

Figure 4 shows the **Kendall’s correlation coefficient** for all DRAM error categories, time windows and system scopes. The coefficients are sorted in ascending order. To increase the visibility in MareNostum experiments, we plot distinct charts for negative and positive (≥ 0) correlation coefficients, while the gap between them indicates the tests that could not be deployed in practice. The corrected error coefficients range are low, with only a handful of experiments that exceed a value of 0.3, see Figure 4a. For the uncorrected errors, depicted in Figure 4b, the coefficients are even lower. Also, in both charts we observe a roughly equal proportion of the positive correlations, and the unexpected negative ones.

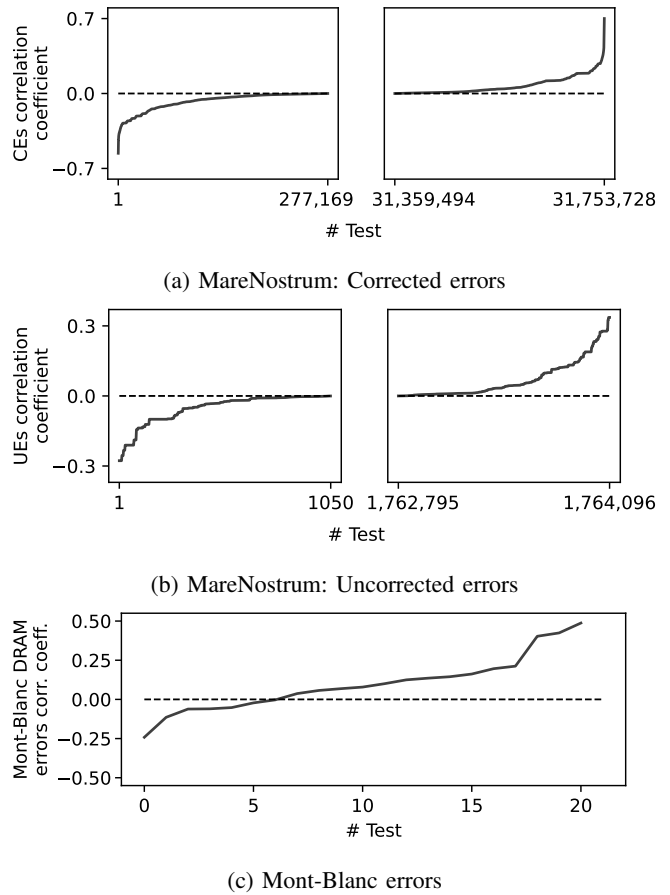
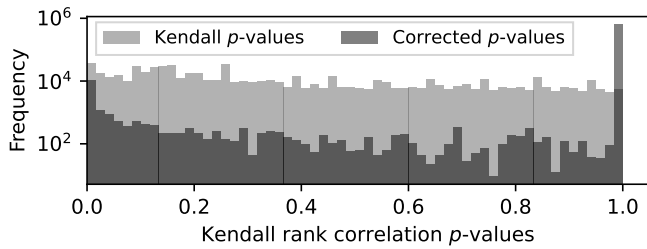


Fig. 4: Most of the correlation tests report low coefficients.

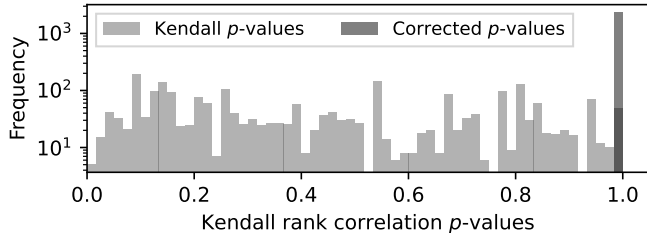
For the **Mont-Blanc prototype**, we test 21 correlations, for three time-windows and seven error types. Their correlation coefficients range from -0.24 to $+0.49$.

To consider the **significance** of the Kendall’s correlation coefficients, we analyze the corresponding **p -values**. Figure 5 depicts the histogram of the p -values provided directly by the Kendall’s test and after the Benjamini–Yekutieli false discovery rate correction [33].

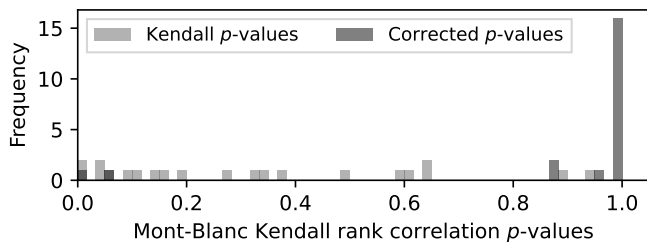
In **MareNostrum** tests, after the correction, p -value = 1 in a vast majority of the CE tests and all UE tests. As the final step of this analysis, we explore the tests that have statistically significant (p -value below 0.05) and moderate or high correlation coefficient. We detect no such tests for transient corrected errors. This is surprising because cosmic ray strikes are frequently considered a plausible cause of these errors [4], [10], [18], [27]. When we analyze the whole CE sample, we find no statistically significant tests with inverse correlations below -0.5 , and only 40 tests with positive correlations above $+0.5$. All of them correspond to the 1 month time window in the 25-months logging period, i.e. the sample of only 25 observations. Out of the 40 tests, 36 are from three DIMMs located in two nodes. All three DIMMs experience higher error rates in the months of the logging period, coinciding with higher neutron counts. However, the recorded errors are



(a) MareNostrum: Corrected errors



(b) MareNostrum: Uncorrected errors



(c) Mont-Blanc errors

Fig. 5: After the false discovery rate correction, p -value = 1 in a vast majority of correlation tests.

repeated, up to thousands of times, on a small number of distinct physical locations (memory cells). Therefore, it is highly unlikely that their underlying cause is an external factor, such as cosmic rays.

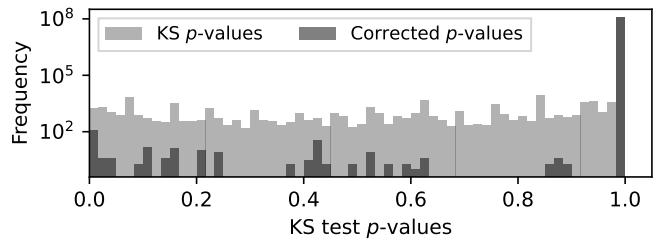
After the false discovery rate correction, only four **Mont-Blanc** tests have p -values below 0.05. All of them correspond to correlation coefficients of 0.13 and 0.14, indicating a low correlation with cosmic rays.

The correlation tests consider the overall trend across all data points and may not reveal a significant association if DRAM errors are more likely to occur only above a certain neutron count threshold. To address this limitation, in the next section we explore the error rates during periods of elevated cosmic ray activity.

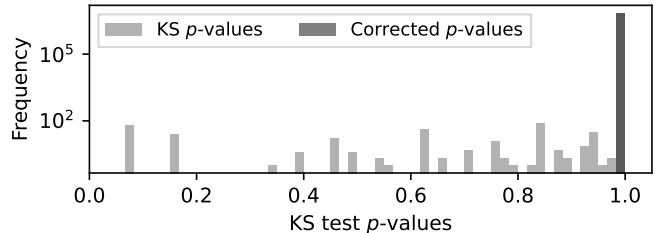
VII. PERIODS WITH THE HIGHEST NEUTRON COUNTS

A. Methodology

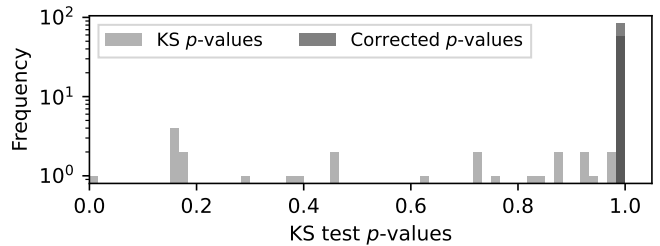
To explore whether DRAM errors are more affected by cosmic rays above a certain neutron count threshold, we partition the DRAM errors into two samples: those observed during high neutron-count periods (above a certain threshold) and the remaining errors. Then we use the Kolmogorov–Smirnov (KS) test [34] to determine whether two DRAM



(a) MareNostrum: Corrected errors



(b) MareNostrum: Uncorrected errors



(c) Mont-Blanc errors

Fig. 6: After the false discovery rate correction, p -value = 1 in a vast majority of correlation tests.

error samples come from the same distribution. Since there is no predefined neutron count threshold which is known to impact DRAM errors, we consider the 90th, 95th, 99th, and 99.9th neutron count percentiles. As in the previous section, we apply the test to all combinations of the error categories, time windows and system scopes listed in Table I and II, and then use the Benjamini–Yekutieli p -value correction.

B. Results

Figure 6 shows the histogram of the p -values provided directly by the Kolmogorov–Smirnov test and after the false discovery rate correction. After the correction, p -value = 1 in all Mont-Blanc and MareNostrum uncorrected error tests. Out of 127,014,912 MareNostrum corrected error tests, we detect 40 statistically significant instances (p -values below 0.05) that exhibit a surprising behavior: lower error rates during the higher cosmic ray activity. The expected behavior, higher error rates during periods with neutron counts above 90th and 95th percentile, is detected in 184 tests. Most of these 184 tests are triggered by only five DIMMs located in three nodes. These DIMMs and the nodes are different from the ones that had a statistically significant correlation with the neutron counts (see Section VI-C). However, they show a similar behavior: they

experience higher error rates in the months with the highest cosmic rays activity, but the errors are periodically repeated on a small number of distinct physical locations. Therefore, it is highly unlikely that their underlying cause are cosmic rays.

VIII. DRAM ERROR PREDICTION

We also explore whether machine learning methods for DRAM error prediction would be enhanced by considering the neutron count measurements.

A. Methodology

We start from random forest model used by Boixaderas et al. [35]. The model predicts **DRAM uncorrected errors (UEs)** based on system metrics and error log information from each DIMM: number of CEs, UEs and UE warnings, number of affected ranks, banks, rows and columns, etc. The model checks the system logs every minute and then predicts whether a UE will occur in a DIMM within the next day. The evaluation is based on a cost–benefit analysis, which compares the system resources needed for training, failure prediction and failure mitigation against the saved compute time due to successful failure prediction and mitigation.

We also use the same random forest model, set of features and methodology to predict the forthcoming **corrected errors (CEs)**. To account for the higher frequency of CEs (compared to UEs) we reduce the prediction window to one hour. The objective of our CE predictions is not to improve the HPC system utilization,⁵ but to investigate whether the neutron counts data enhance the model’s predictive accuracy. If this were the case, it would indicate that the deployed random forest model is capable of detecting subtle relationships between cosmic ray intensity and CE rates; a relationship not captured by the statistical methods analyzed in the previous sections. The CE evaluation is based on the Area Under the Curve (AUC), a standard performance metric used to evaluate the quality of a binary classification model [36]. The metric considers the model’s true positive and false positive rates across various decision threshold settings.

To explore the influence of cosmic rays, we extend the feature set of the original random forest model with the **neutron counts** data. We include the average, standard deviation, and percentage variation of neutron counts over 1 hour, 5 hours, 10 hours, 1 day, 1 week, and 1 month. We split the feature data into 60% for training, 20% for validation and 20% for testing. After training and selecting the best model through hyperparameter tuning, we retrain it using both the training and validation sets before evaluating its final performance on the test set. To determine the significance of neutron count features, we train and evaluate the primary and reference models. The primary models use the **actual neutron counts** information. The reference models use the same data, but with **permuted neutron count** features. This is a standard procedure for assessing feature importance because it maintains the distribution of feature values and ensures the

⁵The CEs do not lead to HPC job failures and lost compute time [35].

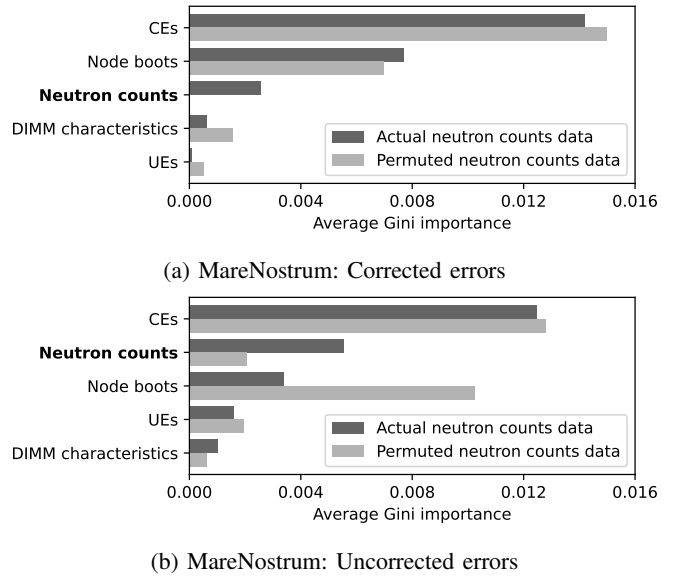


Fig. 7: Gini importance indicates which features are most influential in the model’s predictions.

consistency between primary and reference models [37]. We analyze the predictive capabilities of the models for corrected and uncorrected errors, and use the Gini importance [38] to analyze the significance of the neutron count features.

B. Results

The models that include the actual neutron counts show practically the same prediction performance as the reference models with permuted neutron count features. The primary and reference CE prediction models achieve an AUC of 0.92 and 0.93, respectively. The cost–benefit evaluation of their UE predictions suggest savings of 7451 and 7449 node–hours.⁶

Figure 7 shows the importance of different feature categories, as assigned by the prediction models. Our analysis focuses on the neutron counts group (in bold). In the CE prediction model with actual neutron counts, this feature category is the third most important one (Figure 7a). The reference model appropriately assigns zero Gini importance to these permuted features. The UE models assign even higher importance to the neutron count features (Figure 7b). In the primary model, this is the second most important category, exceeded only by the CE features. Even the reference model puts significant importance to these features. This unexpected model behavior could be related to the instability of the UE prediction model. This is because a small number of uncorrected errors leads to a significant class imbalance that requires considerable

⁶We use the same HPC job logs and cost–benefit calculation as the original study of Boixaderas et al. [35]. The only difference is that we train the model with the majority of the logging data, and test with UEs from the final 20% of the logs. The original study uses time series cross-validation across the entire dataset, starting with smaller datasets at the beginning of the logs and incrementally increasing their size. For this reason, we report a different number of saved node–hours.

undersampling [35], reducing the available information during training and leading to increased model instability.

Overall, CE and UE prediction models using actual neutron counts assign some importance to these features, but they do not perform better than the reference models in which the neutron counts are permuted. The assigned importance could be attributed to the inherent randomness of the models, where the neutron counts may occasionally appear significant in random subsets of the data. This can be observed in Figure 7b, where even randomly permuted neutron counts are given certain importance. Another possibility could be that neutron counts are correlated with another feature, causing the importance to shift to that feature when neutron counts are permuted. However, we discard this possibility by performing correlation tests between each neutron count feature and every other feature, confirming that no such correlation exists. Finally, it is also possible that neutron counts are only important in a very limited set of circumstances, making their impact imperceptible when evaluating the overall model performance.

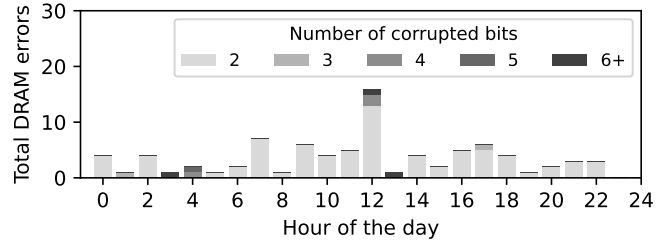
IX. THE SIGNAL AND THE NOISE

In this section we demonstrate why the analysis and methodology we advocate are so important, and what can happen if they are not followed.

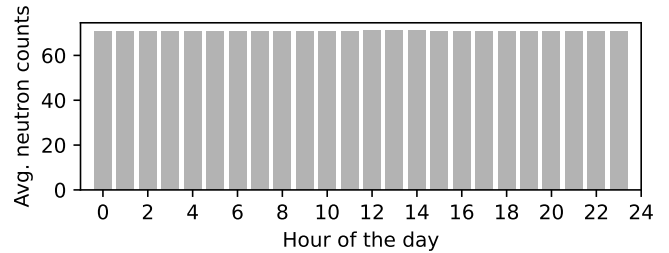
Previous study on the Mont-Blanc DRAM errors “presents evidence which suggests that multi-bit errors are more likely to occur during day time with a high peak when the Sun is at the highest point in the sky” [30]. The authors therefore “suggest that multi-bit memory errors are mostly caused by cosmic rays”. These conclusions are based on the results presented in Figure 8a, which is reproduced from the original paper. The figure plots the total number of multi-bit memory corruptions at a given hour of the day (x -axis), during the observation period from February 2015 to February 2016.

Figure 8b plots the neutron counts recorded by the Guadalajara neutron monitor in the same period. Unsurprisingly, we detect no variation in cosmic ray intensity depending on the time of the day. We get the same results for the complete operational neutron monitor data spanning from 2012 to 2024. This is simply because the position of the Sun on the sky does not impact the rates of cosmic rays that could cause DRAM errors.

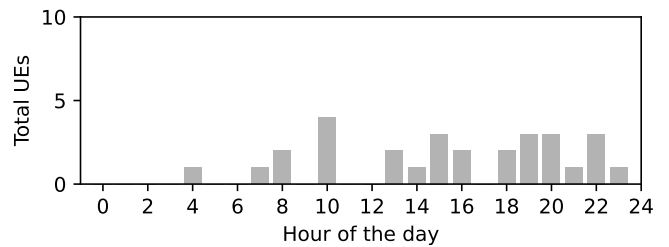
For comparison, we also plot the hour-of-the-day for MareNostrum errors between February 2015 and February 2016. In this period, we detected 29 uncorrected errors (Figure 8c). We also plot the hour-of-the-day chart for all corrected errors (Figure 8d) and the transient ones (Figure 8e). For all CEs, we detect a clear peak at 9h, while the largest number of transient CEs is detected at 18h. To illustrate how a small number of DIMMs can change the general trend of the data, we remove 1% of the DIMMs with the highest number of errors. These results are shown with darker narrow bars in Figures 8d and 8e. We still detect some variation between the time of the day, but some of the highest error rates are now recorded in different hours. We repeated the same analysis with our full logs covering the period October 2014



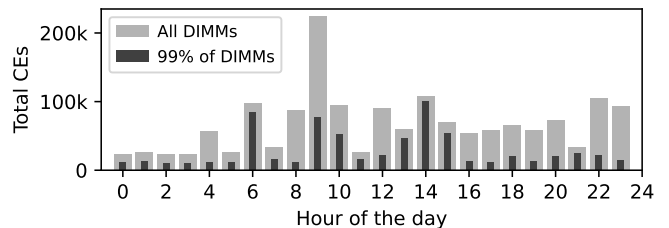
(a) Mont-Blanc errors. Reproduced from the original study [30].



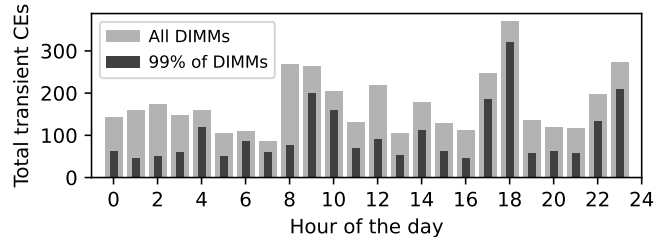
(b) Cosmic rays



(c) MareNostrum: Uncorrected errors



(d) MareNostrum: Corrected errors



(e) MareNostrum: Transient corrected errors

Fig. 8: The neutron counts do not vary between different hours. DRAM error variations cannot be explained with cosmic rays intensity.

to November 2016. These results are not displayed, but the conclusions are the same.

Our results show that DRAM error rates can be volatile even after long periods of logging on large-scale systems [9]. Therefore, although in many research areas bare-eye analysis of the charts might be sufficient, in this particular domain, it will almost certainly lead to unreliable results and incorrect conclusions. The best way to overcome this problem is to use formal statistical methods. The methods that we advocate and deploy are simple to understand and implement, reliable and widely accepted in the statistical community. In addition to the extensive methodology, we describe the underlying sources of cosmic rays, explain which particles should be observed, and provide pointers to publicly-available logs from reliable measurement facilities. We hope that the shared resources and presented methodology will become a standard for any future analysis of the relationship between cosmic rays and DRAM errors in the field. Also, numerous past studies on DRAM errors can (and should) be revisited and extended with this analysis.

X. RELATED WORK

Many recent studies have presented extensive **quantitative analyses of DRAM errors in the field**. The studies analyze error rates and correlate them with chip capacity, temperature, utilization, aging and DIMM generation [3]. The papers also distinguish between the transient (soft) and non-transient (hard) errors [4], [10], and consider the position of the DRAM device in the data-center [16] and the error position in the chip [5], [9], [16], [18], [27], [39].

It is widely accepted that cosmic rays are a plausible cause of DRAM errors in datacenters [2], [3], [9]–[15], [35], [40]. Also, cosmic rays are frequently used as an explanation for some aspects of the observed DRAM error behaviors [12], [16]–[18], [30]. Schroeder and Gibson [17] analyze error logs of 22 HPC systems that were in production use at Los Alamos National Laboratory between 1996 and 2005. The authors detect high DRAM error rates, and suggest that part of the problem could be high altitude of the cluster, which makes it more exposed to cosmic rays. Das et al. [12] analyze the root causes of failures in peta-scale HPC clusters between 2014 and 2016. For some failures, the system logs have insufficient information and show no prior symptoms. The authors, therefore, suspect that a potential cause of these failures could be solar flares or rare cosmic radiations. Sridharan et al. [16] analyze DRAM and SRAM errors from two supercomputers located at Los Alamos National Lab (7320 feet altitude) and Oak Ridge National Lab (850 feet altitude). The high-altitude Los Alamos facility reports significantly higher SRAM error rates. The authors consider that this finding is sufficient to conclude that the majority of observed SRAM faults are caused by cosmic ray strikes. The authors also suggest that cosmic rays are another possible cause of the elevated fault rates in the higher rack chassis. The follow-up study [18] from the same HPC facility concludes that some (but not all) DRAM devices are susceptible to transient faults from

cosmic rays, and that this susceptibility highly varies by device manufacturer. All these studies consider cosmic rays to be an intuitive hypothetical cause of DRAM errors in the field. However, none of them tests this hypothesis.

A quantitative correlation between DRAM error rates and cosmic rays intensity is performed only by El-Sayed and Schroeder [19]. The study analyzes error logs from HPC clusters at Los Alamos National Lab with the objective to discover the factors that influence the HPC system reliability. One out of many factors under study is the cosmic radiation. The authors visually analyze monthly probability of a uncorrected DRAM error as a function of the monthly average neutron counts reported by a neutron monitor located 400km north from the national lab. The results suggest that cosmic rays are not associated with higher uncorrected DRAM error rates. Actually, the results suggest the opposite trend — the higher the neutron counts, the lower the number of errors. The authors find this unexpected and provide one possible explanation for it: while increased rates of cosmic rays might lead to a higher number of corrupted bits, the types of corruption caused by those events might usually be corrected with the error correction codes. This reasoning is aligned with the idea that transient errors typically lead to a single-bit data corruption [10]. We agree that contemporary error correcting codes, capable to correct up to 4 corrupted bits in a 72-bit word, would probably correct a vast majority of the transient errors caused by an external radiation. For this reason, we extend the study of El-Sayed and Schroeder with analysis of the corrected and transient corrected errors. Also, apart from the visual correlation, we apply formal statistical tests and analyze the reported correlation coefficients and their statistical significance. We also use statistical tests to explore whether the error rates have different distributions during periods of elevated cosmic ray activity, e.g. above 90th or 99th neutron count percentile. We perform a vast number of tests that cover all combinations of the error categories, time windows and system scopes. Finally, we analyze in detail all tests that showed statistical significance.

Machine learning methods predict DRAM errors based on the error history, device characteristics (e.g. manufacturer and technology), sensors that monitor the system (e.g. temperature), and workload properties (e.g. memory bandwidth utilization) [2], [15], [35], [40]–[50]. To the best of our knowledge, our study is the first one to explore whether considering the neutron count measurements would enhance these prediction methods.

XI. CONCLUSIONS

In this paper we describe the underlying sources of cosmic rays, explain which particles should be observed, and point to publicly-available logs from reliable measurement facilities. Then we analyze cosmic rays and DRAM errors of two HPC clusters located in Barcelona, 100 meters above the sea level. We explore correlations between cosmic ray intensity and the number of DRAM errors, and apply statistical tests to study whether the error rates have different distributions during

periods of elevated cosmic ray activity, e.g. above 90th or 99th percentile. The exploration covers a vast number of tests that include numerous error categories, time windows and system scopes. We also examine whether machine learning methods for DRAM error prediction would be enhanced if they considered the neutron count measurements.

For the two HPC systems under study, we detect no apparent correlation between DRAM errors and cosmic rays, and no error rate increment even during periods with the highest cosmic ray intensity. We also see that considering neutron counts does not improve DRAM error predictions. In addition to this, we apply the presented methodology to verify the findings from previous studies which claim that some DRAM errors are mostly caused by cosmic rays. We show that these results are unreliable and the conclusions incorrect. Overall, we detect no indications that cosmic rays have any influence on DRAM errors. To understand whether the findings are specific to the systems under study, the analysis should be repeated on other HPC clusters, especially the ones located on higher altitudes. Additionally, the analysis can (and should) be applied to revisit and extend numerous previous studies that use cosmic rays as a hypothetical explanation for certain aspects of the observed DRAM error behaviors. Overall, our study motivates, guides and enables a future research on the frequently mentioned, but insufficiently studied relationship between cosmic rays and DRAM errors in the field.

REFERENCES

- [1] HP, "How memory RAS technologies can enhance the uptime of HPE ProLiant servers," Hewlett Packard Enterprise, Technical white paper 4AA4-3490ENW, Feb 2016.
- [2] I. Giurgiu, J. Szabo, D. Wiesmann, and J. Bird, "Predicting DRAM Reliability in the Field with Machine Learning," in *ACM/IFIP/USENIX Middleware Conference: Industrial Track*, 2017.
- [3] B. Schroeder, E. Pinheiro, and W.-D. Weber, "DRAM Errors in the Wild: A Large-scale Field Study," in *International Joint Conference on Measurement and Modeling of Computer Systems (SIGMETRICS)*, 2009.
- [4] A. A. Hwang, I. A. Stefanovici, and B. Schroeder, "Cosmic rays don't strike twice: understanding the nature of DRAM errors and the implications for system design," *ACM SIGPLAN Notices*, 2012.
- [5] M. V. Beigi, Y. Cao, S. Gurumurthi, C. Recchia, A. Walton, and V. Sridharan, "A Systematic Study of DDR4 DRAM Faults in the Field," in *International Symposium on High-Performance Computer Architecture (HPCA)*, 2023.
- [6] C. Lage, D. Burnett, T. McNelly, K. Baker, A. Bormann, D. Dreier, and V. Soorholtz, "Soft error rate and stored charge requirements in advanced high-density SRAMs," in *International Electron Devices Meeting*, 1993.
- [7] T. J. O'Gorman, "The effect of cosmic rays on the soft error rate of a DRAM at ground level," *IEEE Transactions on Electron Devices*, 1994.
- [8] J. F. Ziegler, H. W. Curtis, H. P. Muhlfeld, C. J. Montrose, B. Chin, M. Nicewicz, C. Russell, W. Y. Wang, L. B. Freeman, P. Hosier *et al.*, "IBM experiments in soft fails in computer electronics (1978–1994)," *IBM journal of research and development*, 1996.
- [9] D. Zivanovic, P. E. Dokht, S. Moré, J. Bartolome, P. M. Carpenter, P. Radojković, and E. Ayguadé, "DRAM Errors in the Field: A Statistical Approach," in *International Symposium on Memory Systems (MEMSYS)*, 2019.
- [10] X. Li, M. C. Huang, K. Shen, and L. Chu, "A Realistic Evaluation of Memory Hardware Errors and Software System Susceptibility," in *USENIX Conference on USENIX Annual Technical Conference (USENIXATC)*, 2010.
- [11] S. Gupta, T. Patel, C. Engelmann, and D. Tiwari, "Failures in Large Scale Systems: Long-term Measurement, Analysis, and Implications," in *International Conference for High Performance Computing, Networking, Storage and Analysis (SC)*, 2017.
- [12] A. Das, F. Mueller, and B. Rountree, "Systemic assessment of node failures in HPC production platforms," in *International Parallel and Distributed Processing Symposium (IPDPS)*, 2021.
- [13] S. Levy, K. B. Ferreira, N. DeBardeleben, T. Siddiqua, V. Sridharan, and E. Baseman, "Lessons Learned from Memory Errors Observed over the Lifetime of Cielo," in *International Conference for High Performance Computing, Networking, Storage, and Analysis (SC)*, 2018.
- [14] X. Du, C. Li, S. Zhou, X. Liu, X. Xu, T. Wang, and S. Ge, "Fault-Aware Prediction-Guided Page Offlining for Uncorrectable Memory Error Prevention," in *International Conference on Computer Design (ICCD)*, 2021.
- [15] C. Li, Y. Zhang, J. Wang, H. Chen, X. Liu, T. Huang, L. Peng, S. Zhou, L. Wang, and S. Ge, "From Correctable Memory Errors to Uncorrectable Memory Errors: what Error Bits Tell," in *International Conference for High Performance Computing, Networking, Storage and Analysis (SC)*, 2022.
- [16] V. Sridharan, J. Stearley, N. DeBardeleben, S. Blanchard, and S. Gurumurthi, "Feng Shui of Supercomputer Memory: Positional Effects in DRAM and SRAM Faults," in *International Conference on High Performance Computing, Networking, Storage and Analysis (SC)*, 2013.
- [17] B. Schroeder and G. Gibson, "A Large-Scale Study of Failures in High-Performance Computing Systems," *IEEE Transactions on Dependable and Secure Computing*, 2010.
- [18] V. Sridharan, N. DeBardeleben, S. Blanchard, K. B. Ferreira, J. Stearley, J. Shalf, and S. Gurumurthi, "Memory Errors in Modern Systems: The Good, The Bad, and The Ugly," in *International Conference on Architectural Support for Programming Languages and Operating Systems (ASPLOS)*, 2015.
- [19] N. El-Sayed and B. Schroeder, "Reading between the lines of failure logs: Understanding how HPC systems fail," in *International Conference on Dependable Systems and Networks (DSN)*, 2013.
- [20] J. F. Ziegler, "Terrestrial cosmic rays," *IBM journal of research and development*, 1996.
- [21] Neutron Monitor Database, "NMDB," <https://www.nmdb.eu/nest/>, accessed: 2024-07-12.
- [22] Monitor de Neutrones de Castilla-La Mancha, "CaLMa," <https://pctclm.com/project/monitor-de-neutrones-de-castilla-la-mancha-calma/>, accessed: 2024-05-16.
- [23] Rome Neutron Monitor, "Rome Neutron Monitor," http://webusers.fis.uniroma3.it/svircio/pag_1.html, accessed: 2024-05-31.
- [24] D. Sierra-Porta, "Cross correlation and time-lag between cosmic ray intensity and solar activity during solar cycles 21, 22 and 23," *Astrophysics and Space Science*, 2018.
- [25] "Partnership for Advanced Computing in Europe (PRACE) Research Infrastructure," <http://www.prace-ri.eu>, accessed: 2023-12-03.
- [26] A. Kleen, "MCELOG: Memory Error Handling in User Space," in *International Linux System Technology Conference (Linux Kongress)*, 2010.
- [27] V. Sridharan and D. Liberty, "A Study of DRAM Failures in the Field," in *International Conference on High Performance Computing, Networking, Storage and Analysis (SC)*, 2012.
- [28] *System x iDataPlex dx360 M4 Types 7912 and 7913: Problem Determination and Service Guide*, IBM, Apr 2014.
- [29] N. Rajovic, A. Rico, F. Mantovani, D. Ruiz, J. O. Vilarrubi, C. Gomez, L. Backes, D. Nieto, H. Servat, X. Martorell *et al.*, "The Mont-Blanc prototype: An alternative approach for HPC systems," in *Proceedings of the International Conference for High Performance Computing, Networking, Storage and Analysis (SC)*, 2016.
- [30] L. Bautista-Gomez, F. Zylkyarov, O. Unsal, and S. McIntosh-Smith, "Unprotected computing: A large-scale study of dram raw error rate on a supercomputer," in *International Conference for High Performance Computing, Networking, Storage and Analysis (SC)*, 2016.
- [31] M. G. Kendall, "A new measure of rank correlation," *Biometrika*, 1938.
- [32] C. D. Christophe Croux, "Influence functions of the Spearman and Kendall correlation measures," *Statistical Methods and Applications*, 2010.
- [33] Y. Benjamini and D. Yekutieli, "The control of the false discovery rate in multiple testing under dependency," *Annals of statistics*, 2001.
- [34] V. W. Berger and Y. Zhou, "Kolmogorov–smirnov test: Overview," *Wiley statsref: Statistics reference online*, 2014.
- [35] I. Boixaderas, D. Zivanovic, S. Moré, J. Bartolome, D. Vicente, M. Casas, P. M. Carpenter, P. Radojković, and E. Ayguadé, "Cost-Aware Prediction of Uncorrected DRAM Errors in the Field," in *International*

Conference for High Performance Computing, Networking, Storage and Analysis (SC), 2020.

- [36] A. P. Bradley, "The use of the area under the ROC curve in the evaluation of machine learning algorithms," *Pattern recognition*, 1997.
- [37] A. Altmann, L. Tološi, O. Sander, and T. Lengauer, "Permutation importance: a corrected feature importance measure," *Bioinformatics*, 2010.
- [38] L. Breiman, "Random Forests," *Machine Learning*, October 2001.
- [39] J. Meza, Q. Wu, S. Kumar, and O. Mutlu, "Revisiting Memory Errors in Large-Scale Production Data Centers: Analysis and Modeling of New Trends from the Field," in *International Conference on Dependable Systems and Networks (DSN)*, 2015.
- [40] I. Boixaderas, S. Moré, J. Bartolome, D. Vicente, P. Radojković, P. M. Carpenter, and E. Ayguadé, "Reinforcement Learning-based Adaptive Mitigation of Uncorrected DRAM Errors in the Field," in *Symposium on High-Performance, Parallel and Distributed Computing (HPDC)*, 2024.
- [41] C. H. A. Costa, Y. Park, B. S. Rosenburg, C.-Y. Cher, and K. D. Ryu, "A System Software Approach to Proactive Memory-Error Avoidance," in *International Conference for High Performance Computing, Networking, Storage and Analysis (SC)*, 2014.
- [42] E. Baseman, N. DeBardeleben, K. Ferreira, S. Levy, S. Raasch, V. Sridharan, T. Siddiqua, and Q. Guan, "Improving DRAM Fault Characterization through Machine Learning," in *International Conference on Dependable Systems and Networks Workshop (DSN-W)*, 2016.
- [43] E. Baseman, N. DeBardeleben, K. B. Ferreira, V. Sridharan, T. Siddiqua, and O. Tkachenko, "Automating DRAM Fault Mitigation By Learning From Experience," in *International Conference on Dependable Systems and Networks Workshops, (DSN-W)*, 2017.
- [44] X. Sun, K. Chakrabarty, R. Huang, Y. Chen, B. Zhao, H. Cao, Y. Han, X. Liang, and L. Jiang, "System-Level Hardware Failure Prediction Using Deep Learning," in *Annual Design Automation Conference (DAC)*, 2019.
- [45] X. Du and C. Li, "Memory Failure Prediction Using Online Learning," in *International Symposium on Memory Systems (MEMSYS)*, 2018.
- [46] B. Nie, D. Tiwari, S. Gupta, E. Smirni, and J. H. Rogers, "A large-scale study of soft-errors on GPUs in the field," in *International Symposium on High Performance Computer Architecture (HPCA)*, 2016.
- [47] B. Nie, J. Xue, S. Gupta, T. Patel, C. Engelmann, E. Smirni, and D. Tiwari, "Machine Learning Models for GPU Error Prediction in a Large Scale HPC System," in *International Conference on Dependable Systems and Networks (DSN)*, 2018.
- [48] L. Mukhanov, K. Tovletoglou, H. Vandierendonck, D. S. Nikolopoulos, and G. Karakonstantis, "Workload-Aware DRAM Error Prediction using Machine Learning," in *International Symposium on Workload Characterization (IISWC)*, 2019.
- [49] X. Wang, Y. Li, Y. Chen, S. Wang, Y. Du, C. He, Y. Zhang, P. Chen, X. Li, W. Song *et al.*, "On Workload-Aware DRAM Failure Prediction in Large-Scale Data Centers," in *VLSI Test Symposium (VTS)*, 2021.
- [50] P. Zhang, Y. Wang, X. Ma, Y. Xu, B. Yao, X. Zheng, and L. Jiang, "Predicting DRAM-Caused Node Unavailability in Hyper-Scale Clouds," in *International Conference on Dependable Systems and Networks (DSN)*, 2022.